Hindawi
Advances in Civil Engineering
Volume 2023, Article ID 7464998, 11 pages
https://doi.org/10.1155/2023/7464998

Research Article

Interference Effect of Closely Spaced Foundation Footing on Settlement Variation

Damtew Melese,[1] **Dekebi Genemo**,[1] **Yada Boru**,[2] **Alemineh Desisa**,[1] **Tigist Mezmur**,[1] **and Mulatu Tamru**[3]

[1]*Faculty of Civil and Environmental Engineering, Jimma Institute of Technology, P.O. Box 378, Jimma 47, Ethiopia*
[2]*Faculty of Civil Engineering, Wroclaw University of Science and Technology, Wybrzeże Wyspiańskiego 27, 50-370 Wroclaw, Poland*
[3]*Department of Civil Engineering, Mizan Tepi University, Tepi, Ethiopia*

Correspondence should be addressed to Damtew Melese; melese0510@gmail.com

Received 23 January 2023; Revised 17 April 2023; Accepted 10 May 2023; Published 22 May 2023

Academic Editor: Luigi Fenu

Industrialization and urbanization have run into situations where the construction of buildings is close to each other. This closeness arises due to the restricted available space in a practical construction manner. Such a situation was a reason for the cause of footing of the same and adjacent structures coming closer. This condition causes interference effects, soil-structure interaction, and the stress zone impact to behave differently other than the continuum soil media in the vicinity under the base of the foundation due to overlap stress distribution, which results in excessive foundation settlement. Therefore, the study aims to assess the interference effect of closely spaced footing on settlement variation. In this regard, comprehensive experimental soil properties were conducted using the American Society for Testing and Materials (ASTM) testing procedures to characterize soil behavior. The interference of two footings in the settlement is studied using 3D finite element analysis. The hardening soil was used to model the foundation soil medium using the Plaxis 3D program. Certain vital factors of two neighboring footings for differing maximum loads, distance, embedment ratio, soil layer, and groundwater level are discovered to impact overlapping footing influence. It is observed that the spacing between the footings increases, and the interference impact on the overlapping footings declines, reaching the isolated footing condition at spacing higher than five foundation footing dimensions and increasing when the spacing between the footings decreases.

1. Introduction

Due to the shortage of available space for construction, rapid urbanization, and high structural demand, a group of foundations may be forced to come up close to another. Because of these phenomena, the stress zones beneath the foundations can overlap, causing distraction and complexity in the footings' failure mechanism, settlement, and bearing capacity responses. In regard to soil types, the distance/spacing between two adjacent foundations has a considerable influence on their settlement and bearing capacity behavior. For several years, researchers [1–8] have studied the interference effect and settlement of closely spaced footings of shallow foundations to avoid risk factors associated with foundation design spacing between footings leading to interference that causes the stress zones below the foundation, causing distraction of the building.

Three zones have developed underneath the shallow foundation: the Rankine passive zone, the radial zone, and the triangular wedges, as shown in Figure 1. However, the settlement value relative to individual footings will change at the ultimate loads. For example, if there is overlap in the radial zone, it is essential to adjust the bearing capacity. Stuart [9] uses the efficiency factor (ζ), a function of the spacing to width of the foundations, and the soil friction angle to determine their interference effects. Since ζ is

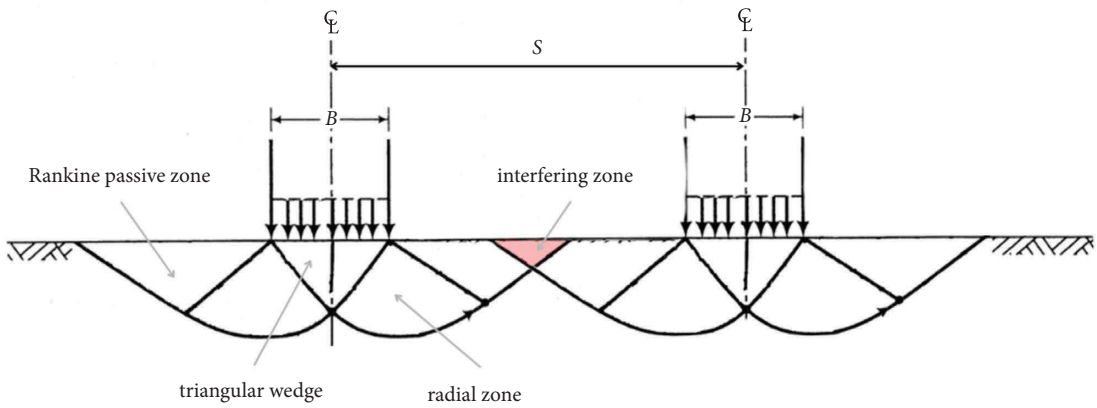

Figure 1: Free scale geometry of adjacent foundation footing model.

greater than one, as the center-to-center spacing between foundations reduces, the ultimate bearing capacity increases; however, the settlement would be more critical than isolated foundations. Stuart's observations do not consider the impact of different parameters (for instance, embedment depth, soils' shear strength, and stiffness parameters).

Analyzing settlement rather than just bearing capacity is more critical in designing the shallow foundation's process. Therefore, settlement estimation is a significant and crucial criterion in the foundation design process. Any structure's efficient design must assure its safety against shear failure and excessive settlement under various loading conditions. Furthermore, building settlements must be kept below acceptable limits at working stress levels. The present study investigates stress interference between two closely spaced footings on a settlement at various working stress levels, using a global safety factor of 2 to 3 that accounts for bearing capacity failure. However, consistent and precise settlement prediction has yet to be achieved using various methods ranging from strictly empirical to complex nonlinear finite elements [10–13]. The most widely used methods were empirical/analytical methods [14–17], experimental methods [2, 18–22], and numerical modeling/finite element methods [19, 20, 23, 24].

Numerical modeling is a powerful mathematical method that allows it to solve imaginable complex engineering problems. A model is a structure or system built to denote a physical concept or phenomenon. The finite element method (FEM) is a well-known numerical analysis technique widely used in civil engineering applications to study and design real-world engineering problems. It has the advantage of more rationally idealizing the material behavior of soil, which is nonlinear with plastic deformations and stress-path dependent. Among the many finite element method algorithms, one of the more popular is Plaxis. Many studies show shallow foundation settlement for interference effect, and settlement of closely spaced footings has been analyzed using Plaxis 2D by considering the Mohr–Coulomb model [25–30]. However, Mohr–Coulomb idealization implies dilation at a constant rate when soil is sheared, which is unrealistic. The normally and lightly over consolidated soil contradict the Mohr–Coulomb idealization since they contains zero angle of dilatancy. While the dilatancy angle is considered as zero, the rate of dilation is also zero not constant rate. Thus, soils on shearing exhibit different stiffness and volume change characteristics depending on preconsolidation pressure, which the Mohr–Coulomb model cannot account for different stiffness directions. This model can predict displacement and failure for general types of soils in various geotechnical applications. Initial soil conditions, such as preconsolidation, play an essential role in soil deformation problems and can also account for the initial stress generation of the hardening soil model. The current finding considers the Hardening soil model in contrast to the Mohr–Coulomb; it accounts for stress-dependency of stiffness moduli and dilation variation. In addition, predicting foundation settlement by the analytical approach has some limitations with complex soil properties. These limitations are minimized by using the finite element method, Plaxis 3D, becoming one of the most applicable worldwide for modeling and analyzing complex geotechnical problems.

2. Materials and Methods

2.1. Soil Sample. The soil samples for the present study were collected during the excavation process from the area of Jimma Town, Ethiopia. An investigation was conducted 346 kilometers south-west of Addis Ababa, at latitude and longitude of 7°40′N, 36°50′E, with an average elevation of 1760 meters above mean sea level. In geological terms, the town is underlain by volcanic rocks of the Tertiary age, which seem to be mostly basalt. The rock unit of the area consists of medium to acid lava and, thus, the so-called trap formation [31].

After removing the topsoil layer, two soil layers were identified: red-brown clay soil with a thickness of 5 m and the second bottom layer in dark grey clay soil with a thickness of 4 m. The soil profile is shown in Figure 2. The laboratory test procedure was performed using the American Society for Testing and Materials (ASTM) standard method. For determination of shear strength parameters, triaxial tests of undisturbed samples were used, whereas disturbed samples were used to conduct index properties tests such as specific

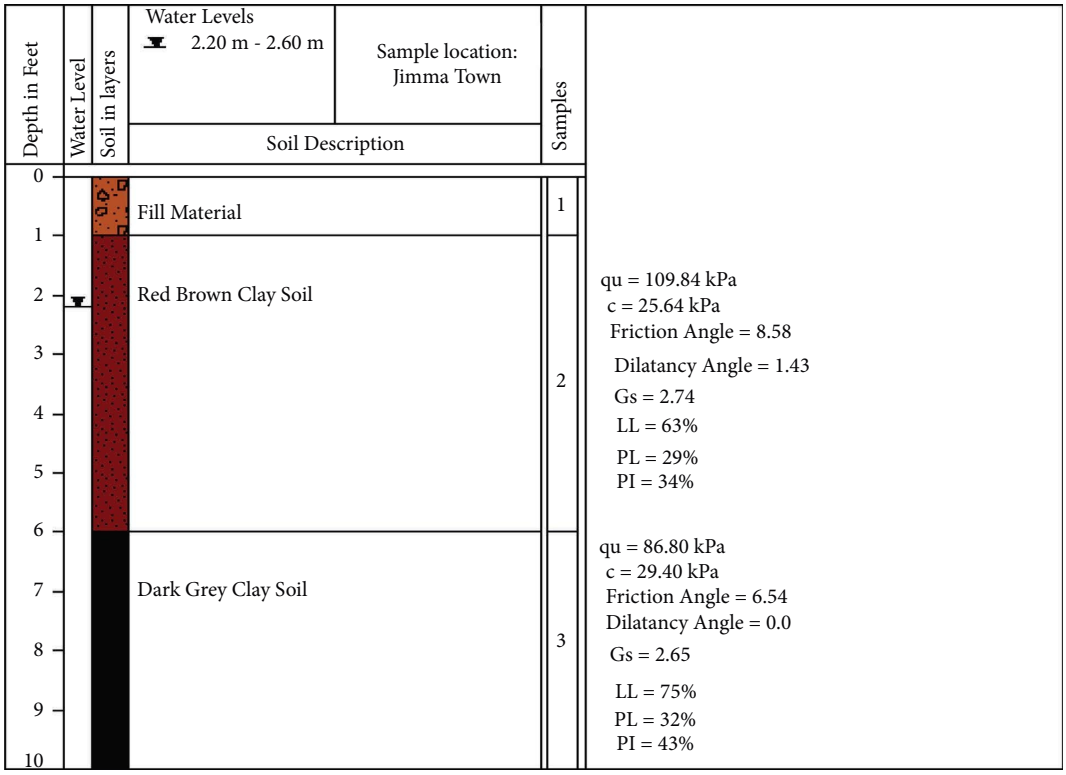

Figure 2: Soil profile and geotechnical properties parameters.

gravity, liquid limit, plastic limit, plasticity index, and grain size analysis. A soil sample was collected from the study area and transported to the Geotechnical Engineering Soil laboratory (Jimma Institute of Technology) and Ethiopian Construction Design and Supervision Works Corporation (Addis Ababa). The detailed soil layers and their engineering properties are demonstrated in Figure 2.

Here, q_u is 109.84 kPa and 86.80 kPa, c is 25.64 kPa and 29.40 kPa, G_s is 2.74 and 2.65, LL is 63% and 75%, PL is 29% and 32%, PI is 34% and 43% for layer 1 (red-brown clay soil), and layer 2 (dark gray clay soil), respectively.

2.2. Soil Model. Based on unconfined compressive strength results, the soil is categorized as medium to stiff clay and medium clay soil for layers 1 and 2, respectively, in this report. The Hardening soil (HS) model is the most effective soil model for medium and stiff soil in their numerical modeling. Therefore, a Hardening constitutive model was chosen to simulate the strain behavior of soils in finite element analysis. The neighboring foundation footings have been extensively studied theoretically and experimentally over the past decades [10, 18, 19, 29]. However, the authors in this study consider hardening soil models for the possible influence of stiffness in a soil mass due to loading, unloading, and stress path history to model soil behavior subject to interference effects of the closely spaced foundation footing. Therefore, Hardening soil models (large numbers of parameters) are appropriate to characterize soil behavior to some extent under several loading conditions. Despite the larger number of parameters, Hardening soil models were supposed to be more representative than elastic or the elastoplastic formulations owing to the stress-strain dependency of stiffness and strength resulting from loading and excavation on the soil beneath the footing (unloading, compression, shearing, and bulging). Available studies verified that a preferable constitutive model that uses a single Young's modulus for different loading orientations and other fixed parameters does not produce adequate simulation results due to the imperfect characterization of the actual variable (stress-path-dependent) soil parameters.

On the other hand, it is critical to use the hardening soil model as the constitutive model in foundation design settlement estimation [32, 33]. These concerns were deemed inclusive due to the hardening soil model considering the stiffness variation under sustained loading conditions with depth and small strains to execute in finite element numerical simulation for geotechnics problems. The hardening soil (HS) model was formulated by the study of [34].

From the triaxial compression tests, according to the (ASTM D2850) procedures, the fundamental parameters extracted are friction angle, soil cohesion (Figure 3), triaxial loading stiffness (E_{50}^{ref}), triaxial unloading stiffness ($E_{\text{ur}}^{\text{ref}}$), and Poisson's ratio ($\nu_{\text{ur}}$).

The modulus in the hardening soil model is described more accurately by three moduli of stress-dependent stiffness moduli by the change of soil stress in the HS model, as described in equations (1)–(3).

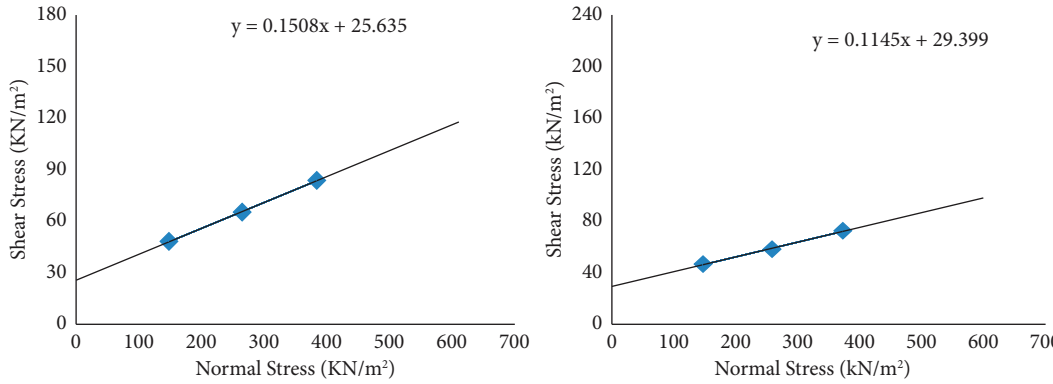

Figure 3: Shear stress vs. normal stress graph (soil layers 1 and 2).

$$E_{50} = E_{50}^{\text{ref}}\left(\frac{c\cos\phi - \sigma_3' \sin\phi}{c\cos\phi + p^{\text{ref}}\sin\phi}\right)^m, \quad (1)$$

$$E_{\text{oed}} = E_{\text{oed}}^{\text{ref}}\left(\frac{c\cos\phi - \sigma_1' \sin\phi}{c\cos\phi + p^{\text{ref}}\sin\phi}\right)^m, \quad (2)$$

$$E_{\text{ur}} = E_{\text{ur}}^{\text{ref}}\left(\frac{c\cos\phi - \sigma_3' \sin\phi}{c\cos\phi + p^{\text{ref}}\sin\phi}\right)^m. \quad (3)$$

In equations (1)–(3), p^{ref} is reference stress for the stiffness and usually set to 100 kPa. E^{ref} is the reference Young's modulus. Plastic soil stiffness parameters E_{50}^{ref} and $E_{\text{ur}}^{\text{ref}}$ are selected and confining pressure is determined from triaxial compression test results. E_{50}^{ref} is calculated as the ratio of 50% deviatoric stress to 50% strain [33] and $E_{\text{ur}}^{\text{ref}} = 3\,E_{50}^{\text{ref}}$. Parameter m is employed in the model to calculate the soil stiffness at any stress level representing power for stress-level dependency. Considering confining pressures, the average values of model parameters $E_{\text{oed}}^{\text{ref}}$ were calculated at $\sigma_3 = 100$ kPa, 200 kPa, and 300 kPa (points on Figure 3) and the average values were presented in Figure 4.

Following this, after thorough visualization, field tests, and laboratory tests, the soil profile bore log characteristics were summarized as presented in Tables 1 and 2.

ψ is the angle of dilation, ν_{ur} is a pure elastic parameter, and the soil lateral earth pressure parameter is represented by K_o^{nc}, an independent input parameter defined as a default setting $K_o^{\text{nc}} = 1 - \sin\phi$. Finally, the average value of the failure ratio $R_f = 0.9$.

2.3. Calculation Method. Numerical finite element analysis was carried out using Plaxis 3D package commercial software to model the interference effect on the foundation footing. The dimensions of the model domain, the characteristics of the soil profile bore log, and the size of the foundation was chosen based on current building practices as reported in the EBCS-7.

The soil layers were modeled by 6-node or 15-node triangular elements available for deformation and stress in the soil Plaxis 2D. The 15-node triangle has a fourth-order interpolation and twelve stress points for displacements. Consequently, the 15-node triangle is more useful for complex problems, but it consumes more memory and performs calculations and operations slightly slower. Therefore, the 15-node elements are more recommended [35, 36].

Plaxis uses data from processed laboratory test results as shown in Table 1; analysis are conducted using a defined soil domain (in the x, y, and z directions), and the footing length is sufficient compared to the width of the problem defined in-plane strain. The finite element meshes' lateral and bottom boundaries were set at $10B$ horizontally and $5B$ vertically from the origin of coordinates. The domain and mesh size has a major impact on the FEM-calculated solutions. Detailed analysis must first be performed to correct the domain and subdivide the preferred domain into a finite number of elements to achieve a convergent solution. As shown in Figure 5, boundaries for the soil domain were chosen at an acceptable long distance away from the edges of the footings on all sides. The vertical boundary is assumed to be unrestricted in the vertical direction but restricted in the horizontal. In both vertical and horizontal directions, the bottom horizontal boundary was restricted.

The typical square foundation placed on layered soil and subjected to vertical load is presented in Figure 6. The thickness of the topsoil layer is 5 m, and the second soil layer is 4 m. At the site, groundwater was encountered at a shallower depth. The groundwater table displayed at the time of boring is located at 2.20 m to 2.26 m below the naturally existing ground surface. Hence, for the model simulation, the depth of the groundwater table is considered and used for software analysis. Several multiple trials were accomplished to compute the settlement at the center of the footings by varying the domain and element sizes.

Loads are an important consideration in any building design because they describe the nature and magnitude of external forces that a structure must withstand to provide acceptable performance over its useful life. The intended use, configuration, and location of a building all affect the projected loads. Therefore, it is critical to apply design loads practically that the soils below the footings need to perceive the load safely. Since, the layer of the soil is in two-layer, the estimated load is expected to extend up to a depth of the next layer in order to consider the second layer of the soil

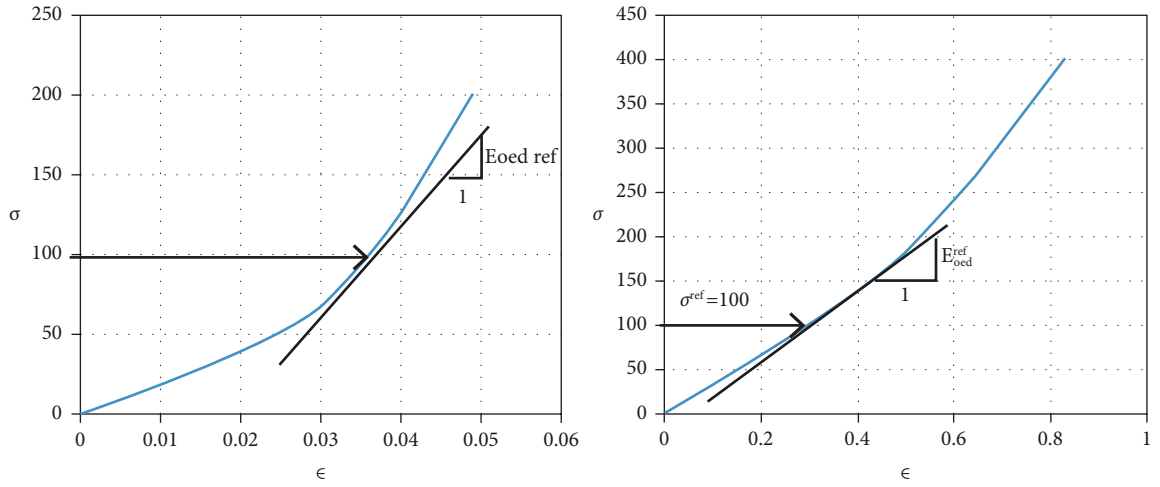

Figure 4: Determination of soil stiffness parameter E^{ref}_{oed} results of an odometer test.

Table 1: Input parameters for the Hardening soil model.

Parameters	Soil type	
	Layer 1	Layer 2
C' (kPa)	25.64	29.40
$\varnothing'$ (°)	8.58	6.54
ψ (°)	1.43	0
E^{ref}_{50} (MPa)	1.864	2.139
E^{ref}_{ur} (MPa)	5.592	6.418
E^{ref}_{oed} (MPa)	3.442	4.515
ν_{ur}	0.2	0.2
M	1.00	1.00
K^{nc}_o	0.990	0.886
R_f	0.9	0.9

Table 2: Structural parameters in numerical analysis.

Parameters	Unit	Values
γ	kN/m^3	24
E	MPa	24
N	—	0.20
Material behavior	—	Linear (isotropic)

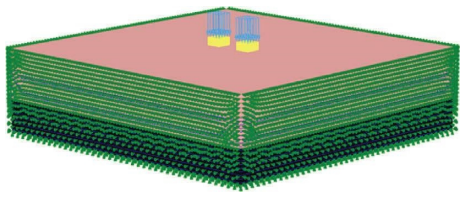

Figure 5: Geometrical fixity of model.

structure within the influence zone. For this case, the load was checked by increasing the second soil layer until subjectized and became optimized to 1000 kN/m^2. In addition, based on this load value, the footing condition has been studied for different cases of footing parametric geometry. The geometry for symmetrical footing was (B = BL (left) = BR (right), and loadings was P = PL = PR). In addition, asymmetric footings have been studied, and asymmetric

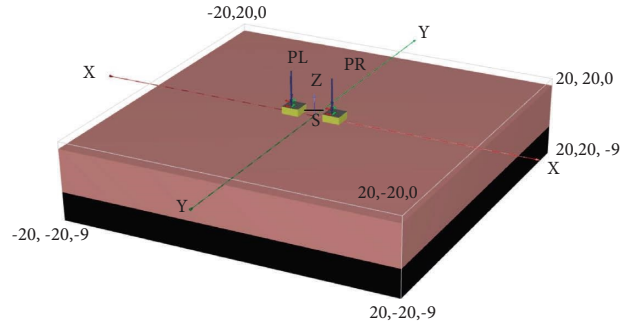

Figure 6: Geometric modeling of soil.

loading (PR = $\beta \times$ PL, where β is the nondimensional parameter) are the two loads that are applied to the width footings on the left and right sides BL and BR (BR = $\alpha \times$ BL, where α is the nondimensional parameter), respectively. The values of nondimensional factors have been changed based on the case study.

The sensitivity analysis was accepted to determine the optimal domain and element sizes beyond which their effect on the computed results is insignificant and thus can be isolated. Depending on the footing geometry and loading, the following conditions are considered: Two closely spaced interfering footings resting on the surface of different soil layers is studied, adopting different trial footing dimension geometry condition.

As the spacing reduces, where the passive zones/radial zone interpenetrates, the interference zones start to interfere as the footings approach each other, and the soil between the individual footings travels down with the footings.

The pressure settlement curves obtained for case asymmetrical footing with asymmetrical loading footings presented in Table 3 show that the bearing pressure of the interfering footing of the left footing decreases by 15.34 to 14.19% at $S/B_L = 0.5$, while the bearing capacity value remains the same as that of the isolated footing at all $S/B_L = 5.0$, indicating that interference has insignificant or no impact on bearing capacity. However, interference had a major impact on the settlement on the left footing and increased from 26%

Table 3: Bearing capacity and settlements of footing for asymmetrical footing and asymmetrical loading.

S/B_L	Bearing pressure @75 mm				δ (mm)			
	$D/B_L = 0.0$ $\alpha = 1.5$, $\beta/\alpha = 2$		$D/B_L = 0.0$ $\alpha = 2$, $\beta/\alpha = 1.5$		$D/B_L = 0.0$ $\alpha = 1.5$, $\beta/\alpha = 2$		$D/B_L = 0.0$ $\alpha = 2$, $\beta/\alpha = 1.5$	
	Left	Right	Left	Right	Left	Right	Left	Right
0.5	157.10	143.49	159.22	134.67	26.67	32.00	45.71	37.95
1.5	167.69	168.43	179.63	201.23	25.71	31.00	28.67	36.97
2.5	178.56	181.77	180.50	206.63	20.95	30.60	23.81	36.61
3.5	184.11	190.40	182.62	211.98	20.00	30.00	20.00	36.00
5.0	185.56	195.65	185.20	212.90	20.00	30.00	20.00	36.00
5.5	185.52	195.200	185.15	212.65	20.00	30.00	20.00	36.00

to 56.25% in the settlement related to the isolated footing when the footing size changed. This means that as asymmetrical loading was applied to two parallel footings at very near spacing, the larger loading settled more and the stress values of the smaller loading changed. As a result, the smaller footings fail toward the larger footing. For the symmetrical cases, the stress values from the left and right footings are almost identical on each other. But, as S/B_L between footings decreases there was overlapping of the stress zones of individual footing. This causes the settlement of footings to be increased when the footings are placed close to each other.

Accordingly, the authors used different conditions of analyses to make a result discussion of parametric studies as discussed in the following subsequent section:

(1) Symmetrical footings and symmetrical loading (S/BL = 0.5, 1.5, 2.5, 3.5.5 and for different depths of footing to width of footing (D/B) = 0.0, 1.0 ($\alpha = 1$; $\beta/\alpha = 1$))

(2) Symmetrical footings and asymmetrical loading ($\alpha = 1$; $\beta/\alpha = 1.25$, 1.50, 1.75, and 2.00)

(3) Asymmetrical footings and symmetrical loading ($\alpha = 1.5$, 2.0; $\beta/\alpha = 1$)

(4) Asymmetrical footings and asymmetrical loading ($\alpha = 1.5$, 2.0; $\beta/\alpha = 1.50$ and 2.00)

(5) Effects of ground water level on footing settlement (2.20 m and 2.60 m)

For this task, a square footing of size 2 m × 2 m, presented in Figure 7, located on the soil model, is considered for the numerical analysis. Hence, the square footing has high bearing pressure, contributing to a more confining impact. However, the footing size and loading under asymmetrical varied based on sensitive parameters in the numerical analysis.

3. Result and Discussion

3.1. Parametric Studies. The parameters for this sensitivity analysis were evaluated based on the varying size of footing and load with correspondence of spacing variation for each case until the failure of soil was obtained to assess the ultimate bearing capacity of the soil. The maximum allowable settlement for isolated footing on clay soil is 75 mm as per IS (1904). The interference effect is analyzed for bearing pressure corresponding to permissible settlement. The settlement effect studied corresponding to the working load of 100 kPa isolated footing also studied that the nonuniform settlement at the base of footings influences the tilting of the footings. The effect of depth difference of footings and groundwater level variation was also studied concerning the spacing ratio (S/B_L) between the footings.

The dimensionless parameter efficiency factor is used to study the effects. The efficiency bearing capacity factor (ζ_γ) is defined as the ratio of the bearing capacity of interfering footing to that of isolated footing when calculating an interfering foundation's bearing capacity (BC).

$$BC \text{ efficiency factor } \left(\zeta_\gamma\right) = \frac{(\text{BC of interfering footing at failure})}{(\text{BC of isolated footing at failure})}, \tag{4}$$

$$\text{Settlement efficiency factor } \left(\xi_\delta\right) = \frac{(\text{Settlement of interfering footing at failure})}{(\text{Settlement of isolated footing at failure})}. \tag{5}$$

The settlement efficiency factor (ξ_δ) is described as the ratio of interfering footing settlement to isolated footing settlement (equation (5)). The tilt ratio (ζ_θ) is calculated by dividing the difference in the settlement between the inner and outer edges by the footing width. The bearing factor, settlement factor, tilting factor, and interaction factors studied in terms of interference effect for the left and right footings are properly labeled, and their values are read from the corresponding axes as defined on the left and right.

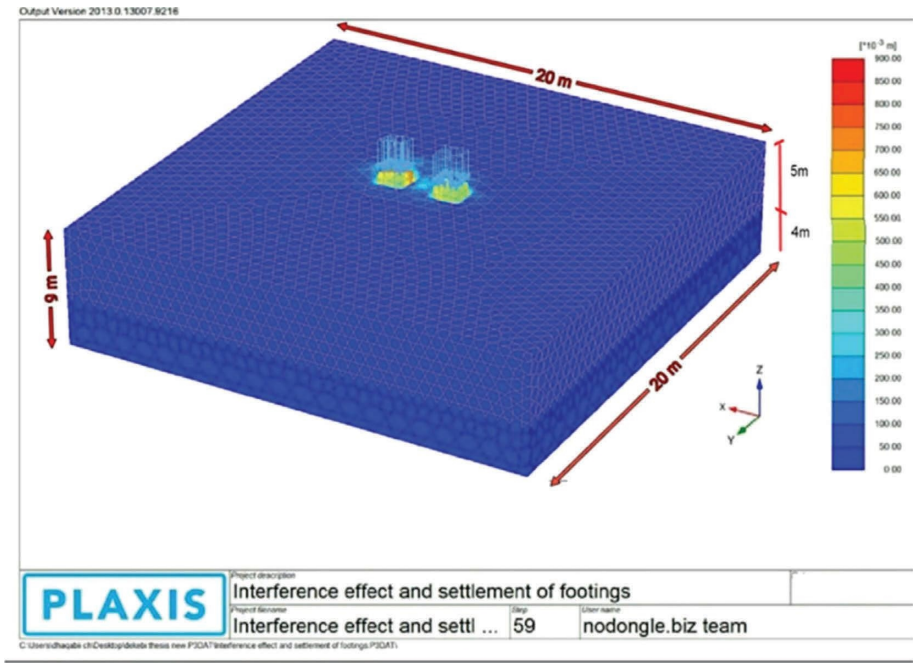

Figure 7: 3D model meshing element.

3.2. Settlement Variation

3.2.1. Symmetric Footing and Symmetric Loading. In symmetrical footing and loading conditions, the load varies with $\alpha = 1.0$, and $\beta/\alpha = 1.0$ and is shown in Figure 8 of the settlement variation. It was observed that for the symmetrical footing and symmetrical loading, as the spacing ratio S/B_L increases, the interference settlement decreases and becomes one when the spacing between footings is far as spacing ratio $S/B_L \geq 5.0$. This result indicates the footings act as individual footing when footings are far apart as a clear spacing ratio $S/B_L \geq 5.0$. The settlement interference is increased by 33% as compared with isolated footing.

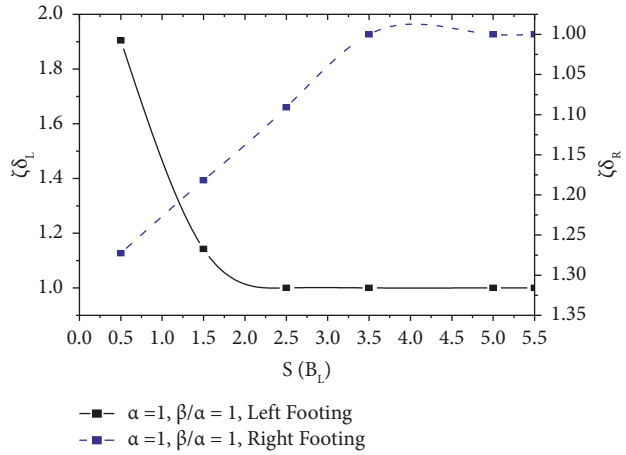

Figure 8: Settlement efficiency factor with varying spacing at $\alpha = 1$ and $\beta/\alpha = 1$.

3.2.2. Symmetrical Footings and Asymmetrical Loading. Figure 9 shows the variance of settlement factors concerning spacing ratio. The plots for $\beta/\alpha = 1.0$ reflect symmetrical footing and symmetrical loading, while the rest of the plots represent symmetrical footing and asymmetrical loading. It was observed that when asymmetrical loads are applied, the larger load settles down more and interferes with the smaller load. As the S/B_L ratio increases, the interaction factors decrease, eventually reaching a constant value of one at greater spacing $S/B_L \geq 5.0$, and while comparing with symmetrical footing and symmetrical loading, the interaction factors of the left footing are equal to the interaction factors of the right footing for $\alpha = 1.0$ and $\beta/\alpha = 1.0$. It was also observed that the settlement interference was increased to 44.44% at $S/B_L = 0.5$ while the footings were symmetrical footings and asymmetrical loading.

3.2.3. Asymmetrical Footings and Symmetrical Loading. In Figure 10, the results were obtained for footing that is with asymmetrical footing size and symmetrical footing load. The interaction factors for the left footing are greater than the interaction factors for the right footing at a specified S/B_L ratio, with an increase in the width of the right footing compared to the width of the left footing. Thus, the smaller footing size interferes with the larger footing size when the footings were close to each other. As S/B_L ratio increases, the interaction factors decrease and reach a value of unity, where the footings are considered to be behaving as an isolated footing. When footing size was asymmetric, the settlement interference was increased to 41.18% at $S/B_L = 0.5$.

3.2.4. Asymmetrical Footings and Asymmetrical Loading. Figure 11 presents the variation of the interaction factors with S/B_L for asymmetrical footing ($\alpha = 1.5$) and asymmetrical loading ($\beta/\alpha = 1.5$ and 2.0). It is observed that the

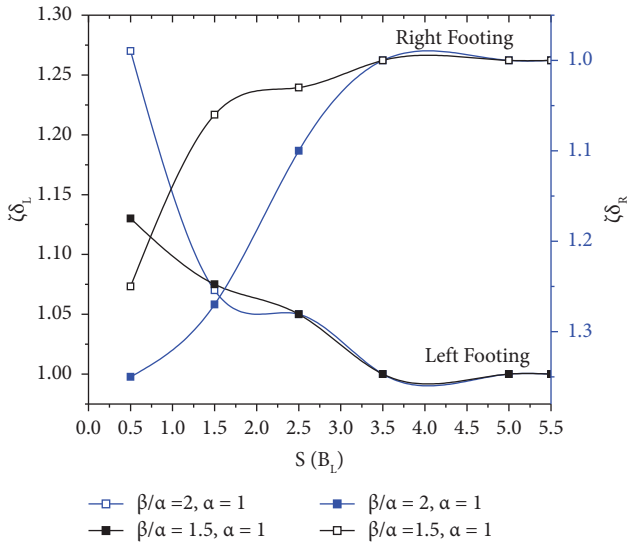

Figure 9: Variation of the settlement factors with S/B_L for; $\alpha = 1.0$ and $\beta/a = 1.5$ and 2.

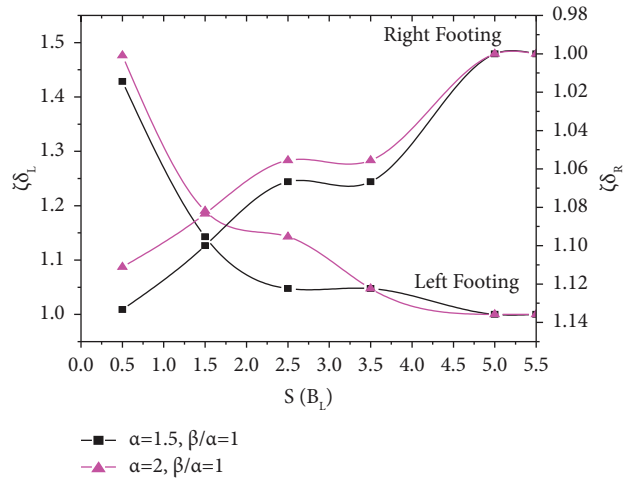

Figure 10: Variation of the settlement factors with S/B_L for; $\alpha = 1.5$, 2; and $\beta/\alpha = 1.0$.

settlement factor decreases as spacing between footings increases. It is maximum at $S/B_L = 0.5$ and become unite at $S/B_L = 5.0$ and more. It indicates that footings act as isolated footing as space between footing far apart as $S/B_L \geq 5.0$. The interaction factors of the left footing increase with an increase in the width of the right footing, according to this study. This is attributable to the fact that a larger footing has a greater impact on a smaller footing.

A similar analysis was carried out for $\alpha = 2.0$, and the interaction factors for the left footing were found to be higher than the interaction factors for the right footing. This may be because the right footing's stress zone interferes significantly with the left footing's stress zone, and vice versa, with the left footing's stress zone resulting in fewer interaction factors for the right footing. Furthermore, as the load intensity on the right footing increases, the zone of impact of the right footing increases resulting in higher interaction factors for the left footing. The interference was increased to 56.25% in

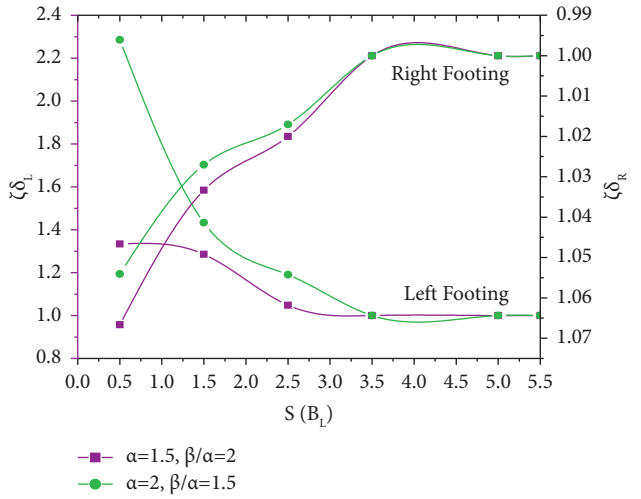

Figure 11: Variation of the tilting factors with S/B_L for; $\alpha = 1.5$, 2; and $\beta/\alpha = 1.5$, 2.

settlement as related to the isolated footing. It was also found that when the spacing ratio between the two footings is 5.0 or more, they act as an isolated footing.

3.2.5. Symmetrical Footings and Asymmetrical Loading at Different Depth-Footing. Figure 12 presents the variations of the interaction factors with S/B_L for asymmetrical footing ($\alpha = 1$) and asymmetrical loading ($\beta/\alpha = 3.0$) when right footing embedded at $D/B_L = 1.0$ and left footing placed at surface $S/B_L = 0.0$. For comparison purposes, the plots of the asymmetrical footing and symmetrical loading ($\alpha = 1.0$, $\beta/\alpha = 3.0$, and $D/B_L = 0.0$) are also presented. In this case, it is obtained that the interference on the settlement is increased from 44.44% to 46.42% when right footing embedded at $D/B_L = 1.0$. Therefore, it is noticed that the interaction factors for left footing while right footing embedded in soil have more interference effect than when two footings are placed at the surface. Like surface footing for the embedded footing, the interaction disappeared at $S/B_L \geq 5.0$.

3.2.6. Asymmetrical Footing and Asymmetrical Loading at Different Depths of Footing. Figure 13 presents the variations of the settlement interaction factors with S/B_L for asymmetrical footing ($\alpha = 1$) and asymmetrical loading ($\beta/\alpha = 3.0$) when right footing embedded at $D/B_L = 1.0$. For evaluation purposes, the asymmetrical footing and asymmetrical loading ($\alpha = 1.5$, $\beta/\alpha = 2.0$, and $D/B_L = 0.0$) are also presented. In this case, it was observed that the interference on settlement on the left footing increases from 45.46% to 47.81% when right footings embedded in soil. Hence, it was considered that the interaction factors for left footing while right footing embedded in soil have more interference effect than when two footings are placed at the surface.

3.2.7. Settlement Variation with Groundwater Tables Variation. Figure 14 shows the interaction factors' variations with S/B_L for symmetrical footing, $\alpha = 1.0$, and

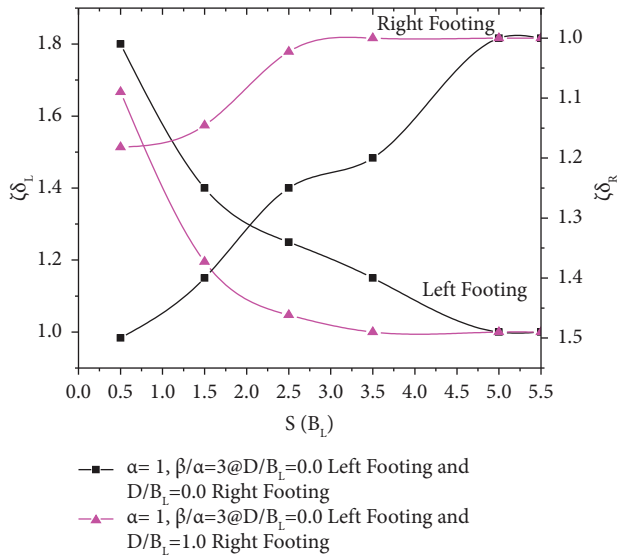

Figure 12: Settlement factor variation when right footing embedded in soil at $D/B_L = 0.0$, 1.0 with S/B_L for $\alpha = 1.0$ and $\beta/\alpha = 3.0$.

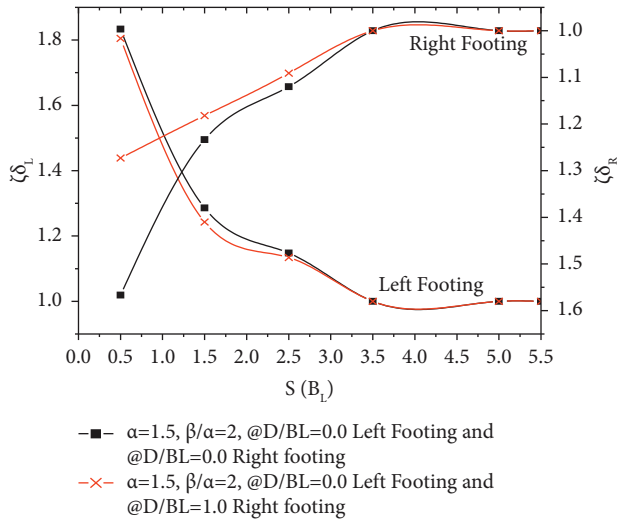

Figure 13: Settlement variation when right footing embedded in soil at $D/B_L = 0.0$, 1.0 with S/B_L for $\alpha = 1.5$ and $\beta/\alpha = 2.0$.

symmetrical loading, $\beta/\alpha = 1.0$, while water tables vary from 2.20 m to 2.60 m for comparison purposes. It obtained that the interference effect of footing at water level increases to the ground level has more effect than during the groundwater far from ground level. In case the effect of interference disappears when the footing is far from each other ($S/B_L \geq 5$) for, the groundwater level is reduced to 2.60 m. However, the settlement of interfering footing increased by 33% and 20% at $S/B_L = 0.5$ when the groundwater level was at 2.20 m and 2.60 m, respectively.

3.3. Summary of Comparing Present Findings with Previous Work. The earlier works by authors [2, 17, 18, 35–37] suggested the influence of interference effects on adjacent footing optimum S/B from 4.5 to 10 range using finite element analysis

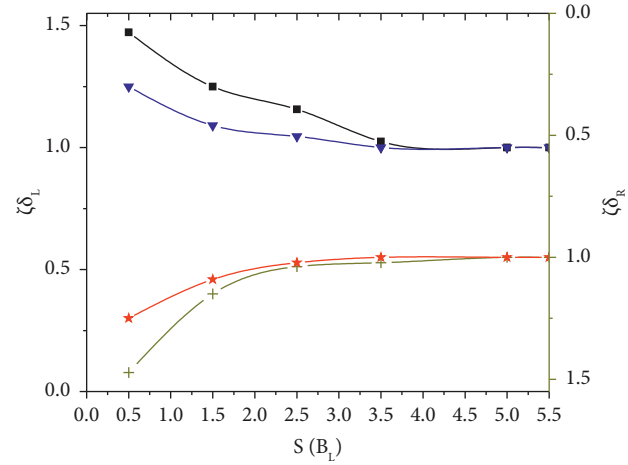

Figure 14: Settlement with groundwater variation.

and experimental works. There is some common sense of agreement with the uncertain reality of specific possible clear distance, soil layers depth, and footing geometry among researchers, which are highly pronounced gaps to figure out by the simple model. As an example, the current study is in good agreement with the effort discovered by authors [10, 36] for the interference of two symmetric closely spaced strip footings resting on the surface of the semi-infinite clay soil medium shows that when the clear spacing $S/B \geq 5$, the efficiency factor for $S/B = 0.5$ is predominant and two footings function as an independent footing. Therefore, the authors in this current work recommend a stochastic approach with an advanced soil model to reach the possible output.

4. Concluding Remarks

Shear strain contours for various scenarios are being examined to understand the failure mechanisms better. It has been established that there is a critical spacing between two adjacent footings at which the footing/s can bear its most pressure. The necessary spacing varies depending on whether the stress is equal and simultaneous or unequal and sequential loading.

(1) Interfering footings settle at a faster rate than isolated footings of the same width and load. The settlement continues to increase as the clear spacing between the footings decreases, and as the clear spacing between the footings increases, the interaction factors drop and gradually become unity, with the influence of interference becoming negligible. The interference effect is about 33% more than the isolated footing.

(2) When loading and size are uneven, the footing with the bigger width and load considerably impacts the footing with the smaller values. The interference effect is about 18.75% more than the footings with the same load and size.

(3) When the footings are in the interference region, the footings can tilt. When footings are close together, the tilt is more significant, and as the spacing increases, the tilt decreases for symmetrical footing and symmetrical loading, the direction of tilting of footings toward each other as spacing between footings near to each other. However, by the spacing between footings, the direction of the tilt of the footings can be reversed. When the larger footing settles, the smaller footing tilts toward the larger footing, causing the right footing to tilt toward the right side.

(4) The interaction factors of the left footing increase as the depth of the right footing increase for different depths of footings. It is increased by 2.35% more than the footings at the same depth when loading and size footings are uneven.

(5) The settlement of the interfering footings is maximum when the spacing between adjacent footings is about $0.5B_L$ and attains a value as isolated footing at greater spacing ($S \geq 5B_L$). The interference effect occurs when the groundwater level far from the footing depth lowers as the distance between the footings increases.

However, when water depth varies from 2.20 m to 2.60 m, the settlement effect reduces from 33% to 20%. Thus, water depth from footing depth has more influence on the interaction of footings.

Data Availability

The data used to support the study are available from the corresponding author upon request.

Conflicts of Interest

All authors certify that they have no affiliations with or involvement in any organization or entity with any financial interest or nonfinancial interest in the subject matter or materials discussed in this manuscript.

Authors' Contributions

ASD, DCG, DTM, and YTB conceptualized the study, proposed the methodology, managed the software, validated the study, formally analysed the study, and carried out the investigation; YTB and DTM gathered the resources; TM, ASD, DCG, DTM, and YTB curated the data; ASD, DCG, DTM, and YTB wrote and prepared the original draft; and YTB, TG, and MT wrote the review and edited. All authors have read and agreed to the published version of the manuscript.

Acknowledgments

The authors were thankful to the Jimma Institute of Technology for their cooperation in providing the necessary support for carrying out this research study.

References

[1] P. Ghosh, P. K. Basudhar, V. Srinivasan, and K. Kunal, "Experimental studies on interference of two angular footings resting on surface of two-layer cohesionless soil deposit," *International Journal of Geotechnical Engineering*, vol. 9, no. 4, pp. 422–433, 2015.

[2] A. A. Lavasan and M. Ghazavi, "Behavior of closely spaced square and circular footings on reinforced sand," *Soils and Foundations*, vol. 52, no. 1, pp. 160–167, 2012.

[3] P. Ghosh and A. Sharma, "Interference effect of two nearby strip footings on layered soil: theory of elasticity approach," *Acta Geotech*, vol. 5, no. 3, pp. 189–198, 2010.

[4] L. S. Nainegali, P. K. Basudhar, and P. Ghosh, "Interference of two asymmetric closely spaced strip footings resting on nonhomogeneous and linearly elastic soil bed," *International Journal of Geomechanics*, vol. 13, no. 6, pp. 840–851, 2013.

[5] M. F. Alwalan, "Interaction of closely spaced shallow foundations on sands and clays: a review," *International Journal of Advanced Engineering Research and Science*, vol. 5, no. 9, pp. 101–110, 2018.

[6] M. Ornek, M. Laman, A. Demir, and A. Yildiz, "Numerical analysis of circular footings on natural clay stabilized with a granular fill," *Acta Geotech Slov*, vol. 9, pp. 61–75, 2012.

[7] L. Nainegali, P. K. Basudhar, and P. Ghosh, "Interference of proposed footing with an existing footing resting on nonlinearly elastic dense and loose cohesionless soil bed," *European Journal of Environmental and Civil Engineering*, vol. 25, no. 14, pp. 2574–2591, 2021.

[8] C. Schmüdderich, A. A. Lavasan, F. Tschuchnigg, and T. Wichtmann, "Bearing capacity of a strip footing placed next to an existing footing on frictional soil," *Soils and Foundations*, vol. 60, no. 1, pp. 229–238, 2020.

[9] J. G. Stuart, "INTERFERENCE BETWEEN FOUNDATIONS," *WITH SPECIAL REFERENCE TO SURFACE FOOTINGS IN SAND*, vol. 12, no. 1, 1962.

[10] M. Ghazavi and P. Fazeli Dehkordi, "Interference influence on behavior of shallow footings constructed on soils, past studies to future forecast: a state-of-the-art review," *Transportation Geotechnics*, vol. 27, Article ID 100502, 2021.

[11] D. V. Griffiths, G. A. Fenton, and N. Manoharan, "Undrained bearing capacity of two-strip footings on spatially random soil," *International Journal of Geomechanics*, vol. 6, pp. 421–427, 2006.

[12] S. Shu, Y. Gao, Y. Wu, and Z. Ye, "Undrained bearing capacity of two strip footings on a spatially variable soil with linearly increasing mean strength," *International Journal of Geomechanics*, vol. 21, no. 2, Article ID 6020037, 2021.

[13] A. A. Lavasan, M. Ghazavi, and T. Schanz, "Analysis of interfering circular footings on reinforced soil by physical and numerical approaches considering strain-dependent stiffness," *International Journal of Geomechanics*, vol. 17, no. 11, Article ID 4017096, 2017.

[14] R. Salgado, A. V. Lyamin, S. W. Sloan, and H. S. Yu, "Two-and three-dimensional bearing capacity of foundations in clay," *Géotechnique*, vol. 54, no. 5, pp. 297–306, 2004.

[15] A. V. Lyamin, R. Salgado, S. W. Sloan, and M. Prezzi, "Two-and three-dimensional bearing capacity of footings in sand," *Géotechnique*, vol. 57, no. 8, pp. 647–662, 2007.

[16] C. Schmüdderich, A. Alimardani Lavasan, F. Tschuchnigg, and T. Wichtmann, "Behavior of nonidentical differently loaded interfering rough footings," *Journal of Geotechnical and Geoenvironmental Engineering*, vol. 146, no. 6, Article ID 4020041, 2020.

[17] R. Shivashankar and S. Anaswara, "Bearing capacity of interfered adjacent strip footings on granular bed overlying soft clay: an analytical approach," *Civil Engineering J*, vol. 7, pp. 1244–1263, 2021.

[18] A. Gupta and T. G. Sitharam, "Experimental and numerical investigations on interference of closely spaced square footings on sand," *International Journal of Geotechnical Engineering*, vol. 14, no. 2, pp. 142–150, 2020.

[19] S. Alzabeebee, "Interference of surface and embedded three strip footings in undrained condition," *Transportation Infrastructure Geotechnology*, vol. 9, no. 2, pp. 250–267, 2022.

[20] S. S. Saraf and S. S. Pusadkar, *Effect of Footing Shapes and Reinforcement on Bearing Capacity of Three Adjacent Footings BT - Construction in Geotechnical Engineering*, M. Latha Gali and P. Raghuveer Rao, Eds., pp. 135–148, Springer Singapore, Berlin, Germany, 2020.

[21] E. Naderi and N. Hataf, "Model testing and numerical investigation of interference effect of closely spaced ring and circular footings on reinforced sand," *Geotextiles and Geomembranes*, vol. 42, no. 3, pp. 191–200, 2014.

[22] S. Salamatpoor, Y. Jafarian, and A. Hajiannia, "Bearing capacity and uneven settlement of consecutively constructed adjacent footings rested on saturated sand using model tests," *International Journal of Civil Engineering*, vol. 17, no. 6, pp. 737–749, 2019.

[23] L. Nainegali and A. G. Ekbote, *Interference of two nearby footings resting on clay medium*, Springer Singapore, Berlin, Germany, 2019.

[24] P. Rao, Y. Liu, and J. Cui, "Bearing capacity of strip footings on two-layered clay under combined loading," *Computers and Geotechnics*, vol. 69, pp. 210–218, 2015.

[25] D. Saadi, K. Abbeche, and R. Boufarh, "Model experiments to assess effect of cavities on bearing capacity of two interfering superficial foundations resting on granular soil," *Studia Geotechnica et Mechanica*, vol. 42, no. 3, pp. 222–231, 2020.

[26] A. Mabrouki, D. Benmeddour, R. Frank, and M. Mellas, "Numerical study of the bearing capacity for two interfering strip footings on sands," *Computers and Geotechnics*, vol. 37, no. 4, pp. 431–439, 2010.

[27] J. Jayamohan, S. Aishwarya, S. R. Soorya, and K. Balan, "Additional settlement of footing due to loads acting on adjacent foundation BT - geotechnics for sustainable infrastructure development," in *Duc Long P*, N. T. Dung, Ed., pp. 1143–1149, Springer Singapore, Berlin, Germany, 2020.

[28] M. Y. Fattah, K. T. Shlash, and H. A. Mohammed, "Experimental study on the behavior of strip footing on sandy soil bounded by a wall," *Arabian Journal of Geosciences*, Springer, vol. 8, no. 7, pp. 4779–4790, 2015.

[29] M. Y. Fattah, K. T. Shlash, and H. A. Mohammed, "Bearing capacity of rectangular footing on sandy soil bounded by a wall," *Arabian Journal for Science and Engineering*, Springer, vol. 39, pp. 7621–7633, 2014.

[30] M. Y. Fattah, K. T. Shlash, and H. A. Mohammed, "Experimental study on the behavior of bounded square footing on sandy soil," *Engineering and Technology Journal, University of Technology – Iraq*, vol. 32, no. 5, pp. 1083–1105, 2014.

[31] W. Fuentes, J. Duque, C. Lascarro, and M. Gil, "Study of the bearing capacity of closely spaced square foundations on granular soils," *Geotechnical & Geological Engineering*, vol. 37, no. 3, pp. 1401–1410, 2019.

[32] M. Kawa and W. Puła, "3D bearing capacity probabilistic analyses of footings on spatially variable c–φ soil," *Acta Geotech*, vol. 15, no. 6, pp. 1453–1466, 2020.

[33] J. M. Pieczyńska-Kozłowska, M. Chwała, and W. Puła, "Worst-case effect in bearing capacity of spread foundations considering safety factors and anisotropy in soil spatial variability," *Georisk: Assessment and Management of Risk for Engineered Systems and Geohazards*, vol. 27, pp. 1–16, 2022.

[34] T. Schanz, P. A. Vermeer, and P. G. Bonnier, "The hardening soil model: formulation and verification," *Beyond 2000 Comput. Geotech*, Routledge, England, UK, 2019.

[35] J. T. H. Wu and S. C. Y. Tung, "Determination of model parameters for the hardening soil model," *Transportation Infrastructure Geotechnology*, vol. 7, no. 1, pp. 55–68, 2020.

[36] R. B. J. Brinkgreve, "Copyright ASCE 2005 69 soil constitutive models evaluation, selection, and calibration," *Geo-Frontiers Congr*, vol. 4, pp. 69–98, 2005.

[37] S. Anaswara, G. S. Lakshmy, and R. Shivashankar, "Interference studies of adjacent strip footings on unreinforced and reinforced sands," *Transportation Infrastructure Geotechnology*, vol. 7, no. 4, pp. 535–561, 2020.